Far East Journal of Mathematical Sciences (FJMS)

http://www.pphmj.com
http://dx.doi.org/10.17654/MS103061017
Volume 103, Number 6, 2018, Pages 1017-1029 **ISSN: 0972-0871**

TIME-DEPENDENT WATER ABSORPTION OF DIFFERENT TYPES OF ROOT-WATER UPTAKE FROM PERIODIC TRAPEZOIDAL CHANNELS

Imam Solekhudin

Department of Mathematics
Faculty of Mathematics and Natural Sciences
Universitas Gadjah Mada
Yogyakarta, Indonesia

Abstract

Time-dependent infiltration problems from periodic trapezoidal channels with water absorption by plant roots are considered. The problems involve four different types of water absorption by plant roots or root-water uptakes. The problems are governed by the Richards equation. To study the problems more conveniently, the equation is transformed into a modified Helmholtz equation. The modified Helmholtz equation, subject to a set of boundary conditions, is solved numerically using a Laplace Transform Dual Reciprocity Method (LTDRM) and a predictor-corrector scheme simultaneously. Using the solutions obtained, numerical values of the water absorption by plant roots are then computed.

1. Introduction

The study of water infiltration in a homogeneous soil has been conducted by a number of researchers. For example, steady infiltration problems have

Received: September 18, 2017; Accepted: November 15, 2017
2010 Mathematics Subject Classification: 76M15.
Keywords and phrases: Laplace transform dual reciprocity method, time-dependent infiltration, root-water uptake, predictor-corrector, modified Helmholtz equation.

been considered by Batu [3], Gardner [6], Philip [7], Pullan and Collins [8], and Solekhudin [12, 13]. Time-dependent infiltration studies have been considered by Lomen and Warrick [10], Warrick [17] and Clements and Lobo [5].

In this paper, we consider a problem involving time-dependent infiltration from periodic trapezoidal channels with four different types of root-water uptake, which is a continuation of the study conducted by Solekhudin [12, 13]. In the previous study, Solekhudin considered corresponding steady infiltration problems. In order to solve the problem, the governing equation, which is a Richards equation, is transformed into a modified Helmholtz equation. The modified Helmholtz equation is then solved numerically using an LTDRM with a predictor-corrector scheme simultaneously. Using the numerical solutions obtained, numerical values of root-water uptake function are computed.

2. Problem Formulation

Referred to Cartesian frame *OXYZ* with *OZ* positively downward consider a homogeneous soil, Pima Clay Loam (PCL). On the surface of soil, periodic trapezoidal irrigation channels are constructed. The cross-sectional perimeter of the channels is $2L$. The channels are completely filled with water. It is assumed that the channels are sufficiently long, and there are a large number of such channels. Between two channels, a row of crops, with roots of depth Z_m and width $2X_m$, are planted. The distance between two adjacent rows of plants is $2(L + D)$. It is assumed that the geometry of the channels and root zone do not vary in the *OY* direction and are symmetric about the planes $X = \pm k(L + D)$, for $k = 0, 1, 2, \ldots$. These descriptions are shown in Figure 1.

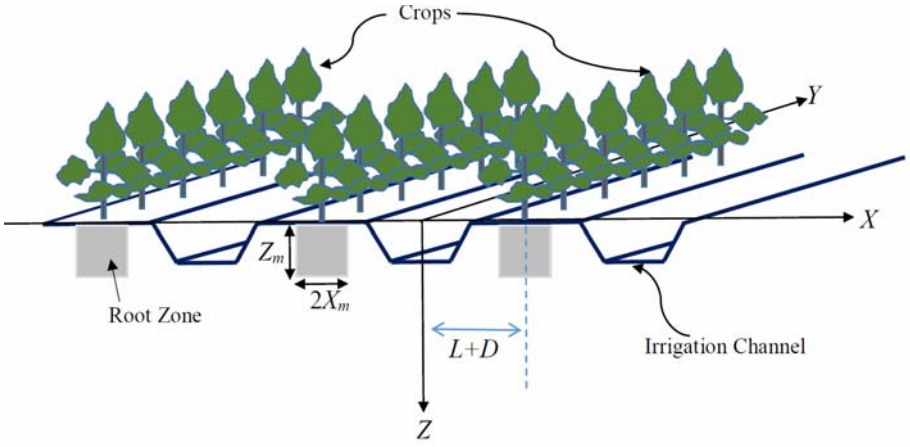

Figure 1. Periodic trapezoidal channels with crops.

Due to the symmetry of the problem, it is sufficient to consider a semi-infinite region defined by $0 \le X \le L + D$ and $Z \ge 0$. The boundary conditions are as used by Batu [3]. In this paper, we consider four different types of root-water uptake, denoted by Root A, Root B, Root C and Root D. These types of roots are as reported by Vrugt et al. [16]. The problem in this study is to determine values of root-water uptake in the soil for infiltration from periodic irrigation channels with different types of root-water uptake.

3. Basic Equations

The geometry of the problems described in the preceding section does not vary in the *OY* direction. Hence, solutions of the problems are independent of the coordinate *Y*. The governing equation of the problems that may be used is

$$\frac{\partial \theta}{\partial T} = \frac{\partial}{\partial X}\left(K\frac{\partial \psi}{\partial X}\right) + \frac{\partial}{\partial Z}\left(K\frac{\partial \psi}{\partial Z}\right) - \frac{\partial K}{\partial Z} - S(X, Z, \psi(X, Z)), \qquad (1)$$

where K is the hydraulic conductivity, θ is water or moisture content in the soil, $\psi(X, Z)$ is the suction potential, and S is the root-water uptake function as in [12, 13], that is

$$S(X, Z, \psi) = \gamma(\psi)\frac{L_t \beta(X, Z) T_{pot}}{\int_0^{Z_m}\int_{L+D-X_m}^{L+D} \beta(X, Z)\, dX dZ}, \tag{2}$$

where L_t is the width of the soil surface associated with transpiration process, β is the spatial root-water uptake distribution, T_{pot} is the transpiration potential, and γ is the root-water stress response function reported by Utset et al. [15]. The spatial root-water uptake, β, is formulated as

$$\beta(X, Z) = \left(1 - \frac{L + D - X}{X_m}\right)\left(1 - \frac{Z}{Z_m}\right) \times e^{-\left(\frac{p_Z}{Z_m}|\, Z^* - Z\, | + \frac{p_X}{X_m}|\, X^* - (L+D-X)\, |\right)},$$

$$\text{for } L + D - X_m \le X \le L + D,\ 0 \le Z \le Z_m.$$

Using the Kirchhoff transformation

$$\Theta = \int_{-\infty}^{\psi} K(t)\, dt, \tag{3}$$

where Θ is the Matric Flux Potential (MFP), an exponential relationship between K and ψ,

$$K = K_s e^{\alpha\psi}, \tag{4}$$

where K_s is the saturated hydraulic conductivity, the suction potential can be formulated as

$$\psi = \frac{1}{\alpha}\ln\left(\frac{\alpha\Theta}{K_s}\right), \tag{5}$$

and equation (1) can be written as

$$\frac{1}{D(\theta)}\frac{\partial\Theta}{\partial T} = \frac{\partial^2\Theta}{\partial X^2} + \frac{\partial^2\Theta}{\partial Z^2} - \alpha\frac{\partial\Theta}{\partial Z} - S(X, Z, \psi(X, Z)). \tag{6}$$

Here $D(\theta) = K(\theta)\partial\psi/\partial\theta$ is the diffusivity, which may be assumed as a constant d in the case of high frequency irrigation [2].

Using the dimensionless variables

$$x = \frac{\alpha}{2}X; \quad z = \frac{\alpha}{2}Z; \quad \Phi = \frac{\pi\Theta}{v_0 L}; \quad u = \frac{2\pi}{v_0\alpha L}U; \quad v = \frac{2\pi}{v_0\alpha L}V;$$

$$f = \frac{2\pi}{v_0\alpha L}F; \quad t = \frac{\alpha^2 d}{4}T \tag{7}$$

yields

$$\frac{\partial\Phi}{\partial t} = \frac{\partial^2\Phi}{\partial x^2} + \frac{\partial^2\Phi}{\partial z^2} - 2\frac{\partial\Phi}{\partial z} - \gamma^*(\Phi)s^*(x, z), \tag{8}$$

where γ^* and s^* are as in [12].

Applying transformation

$$\Phi(x, z, t) = \Phi^*(x, z, t)e^z, \tag{9}$$

into equation (8) yields

$$\frac{\partial\Phi^*}{\partial t} = \frac{\partial^2\Phi^*}{\partial x^2} + \frac{\partial^2\Phi^*}{\partial z^2} - \Phi^* - \gamma^*(\phi)s^*(x, z)e^{-z}. \tag{10}$$

Following Yun [18], in order to apply an LTDRM, we first recast equation (10) to integro-differential form. Using the fundamental solution of Laplace equation

$$\varphi(x, z; \xi, \eta) = \frac{1}{4\pi}\ln[(x-\xi)^2 + (y-\eta)^2], \tag{11}$$

the resulting integro-differential form is

$$\begin{aligned}
&\lambda(\xi, \eta)\Phi^*(\xi, \eta, t) \\
&= \int\int_R \varphi(x, z; \xi, \eta)\left[\Phi^*(x, z, t) + \gamma^*(\Phi)s^*(x, z)e^{-z} + \frac{\partial\Phi^*}{\partial t}\right]dx\,dz \\
&\quad + \int_C \left[\Phi^*(x, z)\frac{\partial}{\partial n}[\varphi(x, z; \xi, \eta)] - \varphi(x, z; \xi\eta)\frac{\partial}{\partial n}[\Phi^*(x, z)]\right]ds(x, z),
\end{aligned} \tag{12}$$

where

$$\lambda(\xi, \lambda) = \begin{cases} 1/2, & (\xi, \eta) \text{ on smooth part of } C, \\ 1, & (\xi, \eta) \in R. \end{cases} \tag{13}$$

Applying Laplace transform

$$\phi(x, z, s) = \int_0^\infty e^{-st} \Phi^*(x, z, t)\, dt, \tag{14}$$

subject to the initial condition

$$\Phi^*(x, z, 0) = 0, \tag{15}$$

on equation (12) yields

$$\begin{aligned} &\lambda(\xi, \eta)\phi(\xi, \eta, s) \\ &= \int\int_R \varphi(x, z; \xi, \eta)\left[(1+s)\phi(x, z, s) + \frac{1}{s}\gamma^*(\Phi)s^*(x, z)e^{-z}\right] dxdz \\ &\quad + \int_C \left[\phi(x, z, s)\frac{\partial}{\partial n}[\varphi(x, z; \xi, \eta)] - \varphi(x, z; \xi, \eta)\frac{\partial}{\partial n}[\phi(x, z, s)]\right] ds(x, z). \end{aligned} \tag{16}$$

It can be seen that there is a non-linear term on the right hand side of equation (16), and hence the direct use of the Laplace transform challenging. To overcome this difficulty, we employ a predictor-corrector scheme. Detailed of the scheme can be obtained in [14].

Integro-differential equation (16) is the integro differential equation of equation

$$\frac{\partial^2 \phi}{\partial x^2} + \frac{\partial^2 \phi}{\partial z^2} = (1+s)\phi + \frac{1}{s}\gamma^*(\Phi)s^*(x, z)e^{-z}. \tag{17}$$

Boundary conditions of the problem in terms of ϕ are:

$$\frac{\partial \phi}{\partial n} = \frac{2\pi}{\alpha L} e^{-z} - n_2 \phi \text{ on the surface of the channel,} \tag{18}$$

$$\frac{\partial \phi}{\partial n} = -\phi \text{ on the surface of soil outside the channel,} \tag{19}$$

$$\frac{\partial \phi}{\partial n} = 0,\ x = 0 \text{ and } z \geq 0, \tag{20}$$

$$\frac{\partial \phi}{\partial n} = 0,\ x = b \text{ and } z \geq 0, \tag{21}$$

$$\frac{\partial \phi}{\partial n} = -\phi,\ 0 \leq x \leq b \text{ and } z = \infty. \tag{22}$$

The term n_2 in Boundary condition (18) is the vertical component of normal vector pointing out region *R*.

Solving equation (17) subject to boundary conditions (18) to (22) employing an LTDRM with a predictor-corrector scheme, we may obtain numerical values of ϕ. These values are then transformed using the Stehfest formula, given as

$$\Phi^*(x,\ z,\ t) \simeq \frac{\log(2)}{t} \sum_{p=1}^{2P} K_n \phi(x,\ z,\ s_n), \tag{23}$$

where

$$s_n = n\frac{\log(2)}{t},$$

$$K_n = (-1)^{(n+P)} \sum_{m=(n+1)/2}^{\min(n,\ P)} \frac{m^P (2m)!}{(P-m)!\, m!\, (m-1)!\, (n-m)!\, (2m-n)!},$$

and *P* is a positive integer, to determine the numerical values of their inverse Laplace transforms, which are the dimensionless MFP.

4. Results and Discussion

In this section, some numerical results of the problem described in Section 2 are presented. As discussed in [12, 13], the homogeneous soil considered in this study is Pima Clay Loam (PCL). The values of α and K_s of the soil are 0.014 cm^{-1} and 9.9 cm/day, respectively [1, 4]. The values of *L* and *D* are the same, that is, 50 cm. The width and the depth of the channels

are $4L/\pi$ and $3L/2\pi$, respectively. The potential transpiration rate, T_{pot}, used in this study is as that used by Li et al. [9], and Šimunek and Hopmans [11], that is, 4 mm/day.

Four different types of root-water uptake models are considered, namely Root A, Root B, Root C and Root D are summarized in Table 1. The root-water stress response function, γ, in this research is as reported by Utset et al. [15], described in Figure 2

Table 1. Parameter values for four different root-water uptake

Root type	fitting parameters					
	Z_m	X_m	Z^*	X^*	p_Z	p_X
Root A	100 cm	50 cm	0 cm	0 cm	1.0	1.0
Root B	100 cm	50 cm	20 cm	0 cm	1.0	1.0
Root C	100 cm	50 cm	0 cm	25 cm	1.0	4.0
Root D	100 cm	50 cm	20 cm	25 cm	5.0	2.0

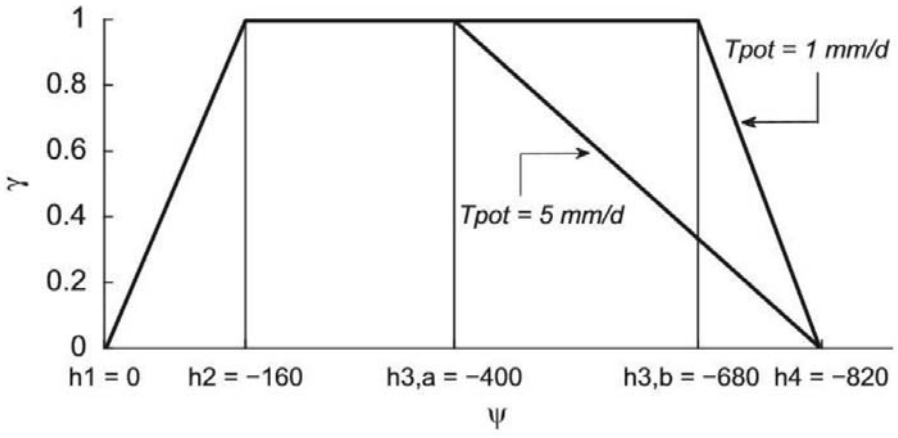

Figure 2. Root-water stress response function, γ.

To obtain numerical results, a DRBEM with a predictor-corrector scheme is employed. To employ the method, boundary is descritized into 404 elements, and 892 interior collocation points are chosen. Some of the results are presented in Tables 2 to 7.

Table 2. Values of root-water uptake, S, at selected locations at $t = 0.8$

Location	Root-water uptake (S)			
	Root A	Root B	Root C	Root D
(60 cm, 20 cm)	0.00102899	0.00112196	0.00117707	0.00284613
(60 cm, 50 cm)	0.00044589	0.00048624	0.00050960	0.00037076
(60 cm, 80 cm)	0.00013346	0.00014554	0.00015250	0.00003339
(75 cm, 20 cm)	0.00386162	0.00420739	0.01085240	0.01441985
(75 cm, 50 cm)	0.00161010	0.00175569	0.00452383	0.00180662
(75 cm, 80 cm)	0.00046638	0.00050865	0.00131058	0.00015747
(90 cm, 20 cm)	0.00882930	0.00961210	0.00551011	0.01336380
(90 cm, 50 cm)	0.00361634	0.00394336	0.00226362	0.00164824
(90 cm, 80 cm)	0.00102869	0.00112198	0.00064475	0.00014117

Table 3. Values of root-water uptake, S, at selected locations at $t = 1$

Location	Root-water uptake (S)			
	Root A	Root B	Root C	Root D
(60 cm, 20 cm)	0.00099747	0.00108744	0.00114085	0.00275817
(60 cm, 50 cm)	0.00042746	0.00046611	0.00048864	0.00035549
(60 cm, 80 cm)	0.00012626	0.00013770	0.00014434	0.00003160
(75 cm, 20 cm)	0.00373873	0.00407475	0.01051695	0.01397193
(75 cm, 50 cm)	0.00154208	0.00168162	0.00433507	0.00173120
(75 cm, 80 cm)	0.00044097	0.00048093	0.00123975	0.00014897
(90 cm, 20 cm)	0.00854134	0.00930642	0.00534326	0.01295665
(90 cm, 50 cm)	0.00346104	0.00377455	0.00216831	0.00157875
(90 cm, 80 cm)	0.00097218	0.00106035	0.00060970	0.00013350

Table 4. Values of root-water uptake, S, at selected locations at $t = 2$

Location	Root-water uptake (S)			
	Root A	Root B	Root C	Root D
(60 cm, 20 cm)	0.00094300	0.00102799	0.00107855	0.00260722
(60 cm, 50 cm)	0.00039555	0.00043129	0.00045225	0.00032903
(60 cm, 80 cm)	0.00011381	0.00012410	0.00013014	0.00002850
(75 cm, 20 cm)	0.00352649	0.00384369	0.00992271	0.01317908
(75 cm, 50 cm)	0.00142503	0.00155389	0.00400714	0.00160028
(75 cm, 80 cm)	0.00039715	0.00043310	0.00111696	0.00013424
(90 cm, 20 cm)	0.00804276	0.00876504	0.00503589	0.01220607
(90 cm, 50 cm)	0.00319493	0.00348417	0.00200256	0.00145802
(90 cm, 80 cm)	0.00087509	0.00095435	0.00054903	0.00012024

Table 5. Values of root-water uptake, S, at selected locations at $t = 3$

Location	Root-water uptake (S)			
	Root A	Root B	Root C	Root D
(60 cm, 20 cm)	0.00093197	0.00101596	0.00106596	0.00257670
(60 cm, 50 cm)	0.00038907	0.00042421	0.00044486	0.00032366
(60 cm, 80 cm)	0.00011126	0.00012132	0.00012723	0.00002786
(75 cm, 20 cm)	0.00348378	0.00379713	0.00980275	0.01301903
(75 cm, 50 cm)	0.00140136	0.00152805	0.00394078	0.00157379
(75 cm, 80 cm)	0.00038821	0.00042334	0.00109189	0.00013123
(90 cm, 20 cm)	0.00794278	0.00865611	0.00497369	0.01205427
(90 cm, 50 cm)	0.00314132	0.00342564	0.00196910	0.00143365
(90 cm, 80 cm)	0.00085531	0.00093276	0.00053667	0.00011754

Table 6. Values of root-water uptake, S, at selected locations at $t = 4$

Location	Root-water uptake (S)			
	Root A	Root B	Root C	Root D
(60 cm, 20 cm)	0.00092897	0.00101269	0.00106253	0.00256840
(60 cm, 50 cm)	0.00038729	0.00042227	0.00044284	0.00032218
(60 cm, 80 cm)	0.00011055	0.00012055	0.00012643	0.00002769
(75 cm, 20 cm)	0.00347219	0.00378448	0.00977020	0.01297559
(75 cm, 50 cm)	0.00139489	0.00152099	0.00392265	0.00156654
(75 cm, 80 cm)	0.00038574	0.00042064	0.00108496	0.00013040
(90 cm, 20 cm)	0.00791566	0.00862655	0.00495682	0.01201309
(90 cm, 50 cm)	0.00312667	0.00340965	0.00195997	0.00142699
(90 cm, 80 cm)	0.00084985	0.00092680	0.00053326	0.00011679

Table 7. Values of root-water uptake, S, at selected locations at $t = 5$

Location	Root-water uptake (S)			
	Root A	Root B	Root C	Root D
(60 cm, 20 cm)	0.00092808	0.00101171	0.00106151	0.00256593
(60 cm, 50 cm)	0.00038676	0.00042169	0.00044223	0.00032174
(60 cm, 80 cm)	0.00011034	0.00012031	0.00012618	0.00002247
(75 cm, 20 cm)	0.00346873	0.00378072	0.00976051	0.00825040
(75 cm, 50 cm)	0.00139294	0.00151887	0.00391720	0.00156437
(75 cm, 80 cm)	0.00038498	0.00041981	0.00108285	0.00013015
(90 cm, 20 cm)	0.00790759	0.00861776	0.00495181	0.01200084
(90 cm, 50 cm)	0.00312227	0.00340484	0.00195723	0.00142499
(90 cm, 80 cm)	0.00084818	0.00092498	0.00053222	0.00011656

Tables 2 to 7 show numerical values of the root-water uptake function, S, at selected locations in the root zone. Table 2 shows values of S at $t = 0.8$. Values of S at $t = 1$, $t = 2$, $t = 3$, $t = 4$ and $t = 5$ are shown in Table 3, Table 4, Table 5, Table 6 and Table 7, respectively. It can be seen that at X = 20 cm, at 20 cm below the soil surface, Root D gives highest value of S. However, the value of S drops rapidly for higher values of X, and the value of S at X = 80 cm is the smallest. It can also be seen that the highest values of S for Root A and Root B are at (90 cm, 20 cm). These results are expected, as the values of the pair (X^*, Z^*) of Root A and Root B are (0, 0) and (0, 20 cm), respectively. Hence, maximum uptakes of Root A and Root B are at positions (100 cm, 0) and (100 cm, 20 cm), respectively. For Root C and Root D, maximum uptakes are at (75 cm, 0) and (75 cm, 20 cm), respectively.

Although not presented in this paper, values of suction potential, ψ, are between $-120 \le \psi \le 0$, and the values of ψ increase as t increases. Hence, values of S decrease as t increases. From Tables 2 to 7, it can be calculated that percentages of decrease from different types of root uptakes are about the same. From $t = 0.8$ to $t = 1$, the decrease in S at Z = 20 cm is about 3%. At Z = 50 cm, S decreases about 4%, and at Z = 80 cm the decrease in S is about 5%.

From $t = 1$ to $t = 2$, the decreases in S at Z = 20 cm, Z = 50 cm, and Z = 80 cm, are about 5%, 7%, and 10%, respectively. Values of S decrease about 1%, 2%, and 2% at Z = 20 cm, Z = 50 cm, and Z = 80 cm, respectively, from $t = 2$ to $t = 3$. From $t = 3$ to $t = 4$, at the same three values of Z, the decreases in S are about 0.3%, 0.5%, and 0.6%, respectively. From $t = 4$ to $t = 5$, the decreases in S are about 0.1%, 0.1% and 0.2%, respectively. These results imply that percentage of the decrease in S declines as t increases. The shallower level of soil reaches steady values of S earlier than those deeper.

5. Concluding Remark

A problem involving time-dependent infiltration from periodic trapezoidal channels with four different types of root uptake has been solved by applying a set of transformations and an LTDRM with a predictor-corrector scheme. The method is applied to obtain numerical values of water absorption by plant roots.

The results indicate that at a fixed level of soil depth, the amount of water absorbed by plant roots is higher than those deeper. The results also indicate that the percentages of decrease in the amount of water absorbed for all the types of root uptake are about the same. The optimum uptake of every type of root uptake depends on parameters X^* and Z^*.

References

[1] A. Amoozegar-Fard, A. W. Warrick and D. O. Lomen, Design nomographs for trickle irrigation system, J. Irrigation Drainage Engineering 110 (1984), 107-120.

[2] H. A. Basha, Multidimensional linearized nonsteady infiltration with prescribed boundary conditions at the soil surface, Water Resour. Res. 35 (1999), 75 -83.

[3] V. Batu, Steady infiltration from single and periodic strip sources, Soil Sci. Soc. Am. J. 42 (1978), 544-549.

[4] E. Bresler, Analysis of trickle irrigation with application to design problems, Irrigation Science 1 (1978), 3-17.

[5] D. L. Clements and M. Lobo, A BEM for time dependent infiltration from an irrigation channel, Engineering Analysis with Boundary Elements 34 (2010), 1100-1104.

[6] W. R. Gardner, Some steady state solutions of the unsaturated moisture flow equation with application to evaporation from a water table, Soil Sci. 85 (1957), 228-232.

[7] J. R. Philip, Steady infiltration from buried point sources and spherical cavities, Water Resour. Res. 4 (1968), 1039-1047.

[8] A. J. Pullan and I. F. Collins, Two and three dimensional steady quasi-linear infiltration from buried and surface cavities using boundary element techniques, Water Resour. Res. 23 (1987), 1633-1644.

[9] K. Y. Li, R. De Jong and J. B. Boisvert, An exponential root-water-uptake model with water stress compensation, J. Hydrol. 252 (2001), 189-204.

[10] D. O. Lomen and A. W. Warrick, Time-dependent linearized infiltration: II. Line sources, Soil Science Society of America Journal 38 (1974), 568-572.

[11] J. Šimunek and J. W. Hopmans, modeling compensated root water and nutrient uptake, Ecol. Model 220 (2009), 505-521.

[12] I. Solekhudin, Water infiltration from periodic trapezoidal channels with different types of root-water uptake, Far East J. Math. Sci. (FJMS) 100(12) (2016), 2029-2040.

[13] I. Solekhudin, Suction potential and water absorption from periodic channels in a homogeneous soil with different root uptakes, Advances and Applications in Fluid Mechanics 20(1) (2017), 127-139.

[14] I. Solekhudin and K. C. Ang, A Laplace transform DRBEM with a predictor-corrector scheme for time-dependent infiltration from periodic channels with root-water up-take, Engineering Analysis with Boundary Elements 50 (2015), 141-147.

[15] A. Utset, M. E. Ruiz, J. Garcia and R. A. Feddes, A SWACROP-based potato root water-uptake function as determined under tropical conditions, Potato Res. 43 (2000), 19-29.

[16] J. A. Vrugt, J. W. Hopmans and J. Šimunek, Calibration of a two-dimensional root water uptake model, Soil Sci. Soc. Am. J. 65 (2001), 1027-1037.

[17] A. W. Warrick, Time-dependent linearized infiltration. I. Point sources, Soil Science Society of America Journal 38 (1974), 383-386.

[18] B. I. Yun, A Laplace transform dual-reciprocity boundary element method for axisymmetric elastodynamic problems, World Academy of Science, Engineering and Technology 6 (2012), 280-286.